

EVALUATING THE THERMAL PERFORMANCE OF
TOPOLOGY OPTIMIZED LOW-COST 3D PRINTED
HEAT SINK MADE OF COPPER.

By

Bilal Taha

THESIS

Presented to the Faculty of the Graduate School of

The University of Texas at Arlington

in partial fulfillment of the requirements

for the degree of

MASTER OF SCIENCE IN MECHANICAL ENGINEERING

THE UNIVERSITY OF TEXAS AT ARLINGTON

MAY 2021

Copyright © by BILAL TAHA 2021

All Rights Reserved



Acknowledgments

I would like to thank my supervising advisor, Dr. Brian Dennis, for letting me be a part of the CFD Lab and the CREST Lab. I am grateful to him for his constant support and guidance throughout my Master's thesis.

I would like to thank my colleagues from the CFD lab and CREST lab for their support. I would also like to acknowledge the effort and contribution made towards my research by Dr. Sandeep Patil and Dr. Fern by helping and guiding me in carrying out my experiments. Their support meant a lot to me as it saved time in carrying out the experiments.

Finally, I would like to express my gratitude to my friend Hasintha for helping me out with CFD simulations. Last but not the least I am grateful to my family for their ceaseless support and love that they have demonstrated through my education and all my life.

Abstract

EVALUATING THE THERMAL PERFORMANCE OF TOPOLOGY OPTIMIZED LOW-COST 3D PRINTED HEAT-EXCHANGER MADE OF COPPER.

Bilal Taha, M.S

The University of Texas at Arlington, 2021

Supervising Professor: Brian H. Dennis

The performance of a heat sink is highly dependent on the overall surface area available for heat transfer. Designing heat sinks with greater surface areas meant bigger size, weight, and volume of heat-exchanger thus making it unfeasible to produce. Design and manufacture of compact-sized heat sinks is a difficult task, as it would require the use of complex surface modeling and complex surface cutting. But with the advent of 3D printing technology, it has become easier to manufacture heat sinks having complex designs producing larger surface areas as they add material layer by layer rather than cutting it away.

The focus of this thesis is to design, manufacture and evaluate the thermal performance of 3D printed heat sinks. A unique method of carrying out thermal topology optimization on cylindrical heat sinks using ANSYS workbench has been discussed. The results from the topology optimization have been used to achieve complex designs. A comparative study was carried out between the topology optimized designs and the conventional straight fin heat sink design to analyze their thermal performance using steady-state thermal analysis. The designs were then 3D printed on a Lultz-Bot 3D printer using a copper-PLA filament. To achieve parts made of pure copper, the

sintering process was carried out and various sintering techniques were explored to combat issues like oxidations, loss of structural integrity, and porosity in the sintered parts. The results from the initial validation study showed that the optimized design performed better. It reduced the heater temperature 12% more than the conventional design. Results from the sintering process showed that the best-sintered parts were achieved when sintering was done in an inert environment at 1070 C and above for longer periods. Lastly, experimental setups were designed using N2 gas tanks, heaters, and cylindrical tubes to simulate the flow of fluid through the heat sink and study its performance. Effective thermal conductivity was calculated and studied. The pressure drop was measured to be around 26 pascals.

Table of Contents

Acknowledgments	3
Abstract	4
Table of Contents	6
List of Illustrations	7
List of Tables	8
Chapter 1 Introduction	9
a) 1.1 Problem Statement	9
b) 1.2 Topology Optimization	10
c) 1.3 Additive Manufacturing	11
d) 1.4 Sintering Process	12
Chapter 2 Literature Review	14
Chapter 3 Methodology	17
a) 3.1 Problem Statement	17
b) 3.2 Topology Optimization	18
a. 3.2.1 3D Model design	20
b. 3.2.2 Validation Study	21
c) 3.3 Additive Manufacturing	24
a. 3.3.1 Copper -PLA	24
b. 3.3.2 3D printer	25
d) 3.4 Sintering	26
a. 3.4.1 Sample Preparation	26
b. 3.4.2 Sintering Process	28
e) 3.5 Experimental setup	33
Chapter 4 Results and Discussion	36
a) 4.1 Results- Topology optimization	36
f) 4.2- Result- Validation study	37
g) 4.3 Results – Additive manufacturing	38
h) 4.4 Results – Sintering	39
i) 4.5 Results – Experimental Setup	43
a. 4.5.1 Calculation of effective thermal conductivities	44
b. 4.5.2 Measuring and Calculating the pressure drop	46
Chapter 5 Summary	48
Chapter 6 Future Works	50
Chapter 7 References	51

List of Illustrations

Fig 1 – Cylindrical Design part for Optimization	17
Fig 2 - Steady State Thermal Analysis	19
Fig 3-Helical Extruded Heat sink	21
Fig 4- Boundary condition on the a) heater b) staigh fin c) topology optimized design	23
Fig 5 - Copper- P LA Filament from Virtual Foundry	25
Fig 6 - Lultz—BOT 3D printer with Spool	26
Fig 7 - Sample Prepared for sintering.	27
Fig 8 - Temperature(y axis) Vs Time (x axis) for open environment sintering	29
Fig 9 - Temperature Vs Time in Vacuum Environment	30
Fig 10 - Crucible for Inert gas sintering	32
Fig 11 a - Temperature Profile Vs time for Inert Environment	33
Fig 11 b- Heat sink inside the HCL	34
Fig 12 - a) Rotameter b) Helium Gas Tank c) Variac	35
Fig 13 - Picture of Setup with a V- manomter hooked up to measure the pressure drop.	35
Fig 14 - Picture of the expreimental Setup a) The blue circlce denote the thermocouple placement b) the red circle denote the heater wire coming out of one end c)The yellow circle denotes the nozzle for N2 supply.	35
Fig 15 - a) Temperature Profile b) Topology optimized results	36
Fig 16 - Temperature distribution a) plain heater b) Heater with straight fin heat sink c)Heater with optimized heat sink	38
Fig 17 - 3D printed on Lultz Bot 3D printer	40
Fig 18 - Sintered parts- From open environment.	41
Fig 19 - Sintered part from Vacuum Furnace	41
Fig 20 - Part Sintered in N2 gas	42
Fig 21 – Sintered part from Helium gas sintering	45
Fig 22 - Effective Thermal Conductivity	45
Fig 23 – V-Manometer Design	47

List of Tables

Table 1 : Boundary Condition for steady state analysis	20
Table 2 : Setup Parameters for Topology optimization	20
Table 3: BC for Steady state thermal analysis for Validation study	22
Table 4: Comparative analysis between both heat sink design	24
Table 5 : Temperature comparison on the heater surfacec in all 3 cases	37
Table 6 : Temperature profile along the test sections @ 7.2 W	43
Table 7 : Temperature Profile along the test section @ 10.5 W	44

Chapter 1

Introduction

1.1 Problem Statement

Heat sinks, and heat spreaders have long been used in the automotive, aerospace, and electronics industries. With improvement in technologies their designs have evolved over time. While designing a heat spreader or a heat sink a major challenge faced by the designer, is the need to improve the total heat transfer rate through a heat spreader while maintaining the size, weight, and dimension of a heat spreader. The performance of any type of heat sink or a heat spreader is dependent on its surface area. Heat spreaders and heat sinks are designed with the intention to maximize the convection area to get the best performance for a given heat sink weight and size. Although the heat transfer process in heat sinks is a complex phenomenon and depends on several factors like fluid velocity, material, fin-type and fin arrangements, etc., it is known that for a set of fixed given conditions the performance of the heat sink depends on the overall surface area.

With the increase in demand for more economical heat sinks, the designers are being encouraged to design heat sinks which are more efficient yet compact in size. The rapid growth in electronic industries has significantly increased the research on low-cost, highly efficient heat sink designs. Similarly, with more companies entering the aerospace industry, the demand for lightweight and compact heat sink design has increased. Apart from that, the communication cable industries alongside the lighting industries are now taking advantage of novel low-cost, compact, and lightweight heat sink designs to compete in the market.

The need for lightweight, compact, and high-performing heat sink design is growing and thus much more research is needed to design and manufacture such types of heat sinks. But designing such high-performance heat sinks (spreader) poses a major issue as increasing the overall surface area for a given volume introduces design complexities.

These complex designs are very difficult to manufacture using conventional manufacturing technologies.

Thus, there is a great requirement to explore and investigate new design methodologies and manufacturing methods that can produce highly complex and compact designs.

1.2 Topology Optimization

There are several methods to achieve a new optimized design. Amongst them topology optimization is quite a famous technique that is used to optimize the material layout within a given design space subjected to some fixed constraints while maximizing the overall performance of a system. In comparison to other optimization techniques like size optimization or shape optimization, the topology optimization technique does not use a predefined configuration. In fact, it operates within a defined design space and puts material in places where it is highly needed and makes sure the constraints are met as well. The topology optimization generally uses finite element analysis (FEA) to evaluate the design performance and the design is optimized using the optimality criteria algorithm.

The application of topology optimization is quite vast. It is majorly used in structural mechanics to attain structures that are lightweight yet have great strength. Such types of designs having higher strength to weight ratio are highly desirable in the aerospace industry where weight and space are both an expensive commodity. The use of topology optimization for heat sink designs has become quite common over the past few years. Many new novel designs have become popular. Conventionally, thermal topology optimization for heat sink design is carried out using self-written codes. These codes are written with an objective function of maximizing the overall thermal conductivity within a given design space while having a mass or volume constraint. The results produced through the topology optimization techniques are quite organic in shape and thus require few manufacturing constraints that are applied so as to achieve designs that can be manufactured. The biggest advantage of using the topology optimization technique is that it enhances the performance (leading to larger surface

areas) while reducing the overall size and weight of a design. In terms of heat sink designs, this means that achieving designs having higher bulk thermal conductivity or higher heat transfer rate while at the same time reducing the overall weight of the heat sink.

In this thesis, we will present a novel method of performing topology optimization on a hollow cylindrical heat sink/heat spreader using ANSYS workbench software.

1.3 Additive Manufacturing

The topology optimized designs are generally quite complex in nature thus cannot be produced by conventional methods. With the advent of additive manufacturing technology, it has become quite feasible to produce such complex designs without any additional cost or time. This is because the conventional machining process requires a careful and detailed analysis of the part geometry, to determine things like what order should the features produced, what material and fixtures must be used for the process[1]. On the contrary, additive manufacturing technology only needs some basic dimensional details and little understanding of the working of AM machines to carry out the manufacturing process. The working of an AM process is such that it uses a layer-by-layer approach of adding material. Each body is cut into small thin cross-sections and the thinner the layer is, the closer the design will be to the original part. Thus for designing complex geometries the conventional processes become quite cumbersome, while it is easy to manufacture using the AM process.

There are many types of AM processes that have been developed over the years. Of the many AM technologies, the Fused Deposition Modeling technique has become quite popular. This is mainly due to their ease of operation and lower cost of FDM printers. Other processes like Selective laser Sintering (SLS) have also been there for a while and have gained popularity in metal 3D printing. The SLS process uses high powered- laser to “sinter” powdered metallic or polymer materials. Sintering is done in a very localized manner with very little energy. In an SLS process, a re-coater applies a thin layer of the powder onto the bed surface where the powdered are sintered according to the geometry of the part being designed. Once one layer is complete, the bed moves

down and another layer of powder is added. There are many advantages of using the SLS process – it requires no supports and the parts are self-supported in the powder bed. It's a very fast process with excellent layer adhesion. But at the same time, the SLS process suffers from issues like that of porosity in parts produced, High shrink rates, and warpage caused due to non-uniform heating, etc. Also, the SLS process is quite expensive. Thus, its use is very limited.

Metal extrusion in additive manufacturing is fairly a new topic. In recent years, metallic FDM printing has picked up some interest. To manufacture parts at a lower cost and in large numbers, the FDM printing technique has great potential. Using metallic filament combined with polymer as a binding agent, the metal FDM process works in a similar manner as the polymer FDM process. These metallic filaments can be used on any standard type FDM printer and can produce parts with great speed and ease. The printed parts coming off the 3D printer are called green parts as they contain the binder material also. The green part then goes through a de-binding process and a sintering process to achieve a part made purely of metal.

The advantages of using such type of process for metal printing is the low cost, ease of setup and maintenance, less expertise required and easy removal of support. Also as the sintering process is carried out separately there is a great control over the mechanical properties of the final part produced.

In this thesis, we will use the FDM/ FFF(Fused Filament Fabrication) technique as the additive process to carry out the 3D printing of the part due to its advantages mentioned above.

1.4 Sintering Process

Sintering is a heat treatment process applied to a powder compact or green parts in order to impart strength and integrity. The green parts produced through the FDM process lacks the strength of pure metals as it contains the binder agent. In order to remove the binder agent from the part, the green part goes through a debinding process. Generally, the debinding process is done either chemically or thermally

depending upon the type of binder material being used. Once the debinding process is complete, the green part is kept inside a furnace for the sintering process. The temperature used in the sintering process is just below the melting point of the metallic part. At this temperature, the diffusion process causes the necks to form which grows to form contact points. The sintering process is highly affected by the environment in which it is carried out. Sintering can be carried out in an open environment but the chances of the parts getting oxidized are very high. Oxidation is a major issue in the sintering process but through judicious choice and zoning of the furnace along with appropriate temperature profile, we can avoid the oxidation process[2].

This thesis talks about solving the issue of designing compact lightweight 3D printed heat sink designs. An optimized design is achieved using the thermal topology optimization technique. The thermal topology optimization was carried out on ANSYS Workbench software in combination with steady-state thermal analysis. The result obtained from the topology optimization technique is used to create a novel 3D printed cylindrical heat-exchanger design which is manufactured using the copper-PLA filament material on a Lultz Bot TAZ 6 FDM Printer. The green part obtained from the 3D printing process were sintered to achieve parts made of pure copper. Various sintering methods are discussed in detail and results from these sintering processes are recorded and compared. Finally, the performance of the heat sink is experimentally measured by calculating the effective thermal conductivity of the part.

Chapter 2

Literature Review

Improvement in the design of heat sinks has always been an active field of research. Due to its application in a large number of fields, several methodologies have been used to carry out design improvements. Many types of optimization techniques have been developed and analyzed, for various applications to achieve heat sink designs that are lightweight and efficient [3][4][5]. Over the past few years, thermal topology optimization techniques have also become quite common to achieve heat sink designs that are lightweight, compact, and efficient. For instance, Alexanderson [6] has performed a density-based topology optimization for 3D heat sinks cooled by natural convection. By assuming the flow to be laminar he presented several optimized designs for grashof's number 10^3 to 10^6 . He concluded by presenting the increase in the number of fin branches by increasing the grashof's number.

In another research- Younghwan Joo et.al. [7] investigated the shape-dependent local variation of heat transfer coefficient, by using a surrogate model, that is usually applied to an arbitrarily shaped structure. He validated the surrogate model and used it to achieve a new novel design. The topology optimized design had 15% less thermal resistance and 26% lesser weight than compared to the conventional heat sink. Conventionally thermal topology optimization is mainly carried out for conduction problems. Conjugate heat transfer thermal topology optimization remains a subject of research due to the complex nature of evolving geometry and boundary layer heat transfer. H . Peter D bock has researched in developing a Hybrid Analytical Thermal Topology optimization(HATTO) approach wherein the solid geometry is optimized discretely with an analytical boundary layer heat transfer profile mapped on the exterior surfaces [8].

Due to the rapid advancement in additive manufacturing (AM) technology complex topology optimized geometries of heat sinks, heat spreaders, and heat sinks can now be produced with great ease. Metal additive manufacturing processes like SLS and Electron beam melting processes have matured enough to produce functional parts ready for use. Z. Gobetz et.al. [9] in a research done for the office of naval research presented a radiator type heat sink design which was manufactured using the SLS process using the EOS MINT 280. In another research Xiang Zhang et.al [10] manufactured gas to gas manifold micro heat sink using the Direct Metal Laser Sintering (DMLS) process with INCONEL 718. He tested it out experimentally and was able to see an improvement of 25% in heat to mass ratio ($Q/mass$) for the parts obtained using DMLS.

Manufacturing heat sinks using the DMLS, EBM, or SLS process can prove out to be quite expensive. Thus, alternative approaches for manufacturing heat sinks have been discovered in the literature. Rachel Ann Felber et.al [11] 3D printed a fin-type heat sink using ABS material and performed experimental analysis to measure its performance by measuring the pressure drop, temperature profile, and air velocity. M. Pelanconi, M. Barbota, and S. Zavattoni [12] have used Stereolithography (SLA) process to produce heat sink models with a large number of lattice structures. They were able to mix alumina powder suspension (42% by volume) into a resin and UC photoinitiators to create a slurry which was thoroughly mixed and given for printing. The green part obtained after 3D printing was then sintered to achieve a part made of pure alumina. The manufacturing approach mentioned in this research paper is like the approach used in this thesis. It has been further extended and a detailed analysis of the sintering process has also been presented.

Sintering of green parts (raw material along with binders. could be metallic material with polymer as the binder) is quite a common technique used in powder metallurgy processes. The same sintering process can be extended to 3D printed parts which are mixed with a binder material. As mentioned above the sintering process generally consists of a debinding phase and a sintering phase. Oyedotun Isaac Ayaani [13] talks in his research thesis about the sintering process of the FDM printed dog bone

structure made of Bronze filament produced by a virtual foundry. The Filament comprised of 90% Bronze and 10% PLA. In his research, the author concluded that the debinding temperature was around 371 C and the sintering temperature was around 832 C, and the hold time for the debinding process was around 90 min while the best results for sintering were observed when the parts were held for 3hrs.

The goal and motivation for this research is that very little research has been done on using characterizing the manufacturing process of 3D printed heat sinks and evaluating its performance experimentally. In this thesis, we will discuss in detail the topology optimization technique used for attaining a thermally optimized design and manufacturing it using FFF/FDM technique. We would also go in-depth to explore the sintering process used to achieve parts made of pure copper. We will discuss the factors affecting the sintering process like 3D printing method, crucible placement, temperature profile, sintering temperatures, and most important of all, the sintering environment. In the end, as a part of the results, we will present a basic comparison between the various methods and their results. Lastly, this thesis also discusses the experimental setup to analyze the performance of the heat sink and characterizing it by calculating the effective thermal conductivity of the part.

Chapter 3

Methodology

In the previous two chapters, we have briefly discussed the topology optimization techniques, FDM metal printing technique, and the importance of correct sintering processes. This chapter will be divided into 5 main sections : (1) Problem Statement (2) Topology optimization (3) Fused Filament Fabrication (FFF)/ FDM (4) Sintering Process (5) Experimental Setup.

The first section explains the problem statement we are trying to solve and why we are solving this problem. The second section discusses in detail about the topology optimization technique, steady-state thermal analysis, and the boundary conditions used. It also discusses, the advantage of carrying out Topology optimization using ANSYS workbench software. The second section describes the process of setting up the part for 3D printing, printing parameters, the effect of various parameters on the final print, and the handling of Copper-PLA filament.

The third section will cover in detail the pre- sintering setup procedures, sintering environments, and post-sintering operations. Lastly, the fourth section discusses the experimental setup procedure for evaluating the experiments.

3.1 Problem Statement

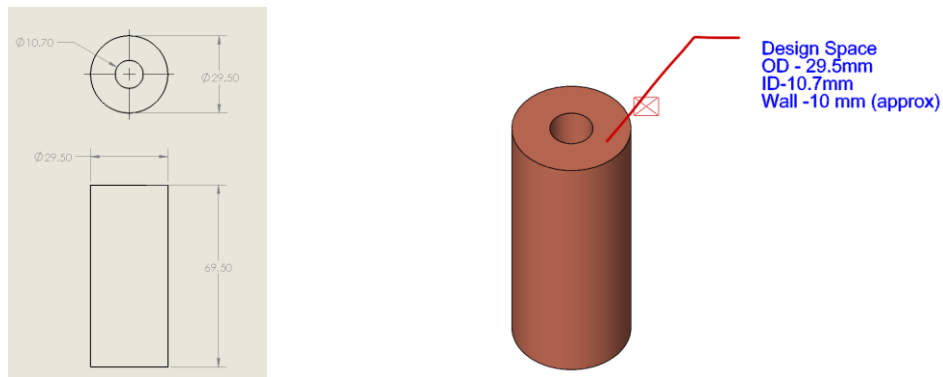


FIG 1 – Cylindrical Design part for Optimization

The problem statement that we had to solve was to design an optimized cylindrical heat sink of 70 mm in length and 30 mm in diameter. Such types of heat sinks can find their application in the LED light industry and communication cooling industry. The hollow cylindrical body was used as a starting point to carry out topology optimization in the design space to achieve an optimal design network of a fin. The heat source (or hot fluid) will be in the center and a network of fins will extract heat from the center(core) and dissipate it to the outer wall and the fluid passing through it.

The Objective of the heat sink here is to lower the temperature of the hot center (core) by removing heat through an optimized fin network. The outer wall will have convective boundary conditions.

3.2 Topology Optimization

To attain an optimized design for the heat sink, we performed a 2D -topology optimization process using ANSYS workbench software. An early assumption was made – that the most dominant direction of the heat transfer would be the radial direction. This was done to simplify our problem which allowed us to carry out thermal topology optimization in 2D design space.

In general the thermal topology optimization method is carried out by writing a self written code to compute the optimized design. The reason for this is that majority of the problems associated with thermal analysis are conjugate problems meaning that they involve both conduction and convection processes. The thermal topology optimization offered by standard software like ANSYS does not incorporate the design dependent loads like convective boundary conditions. This is due to the difficulty in accurately tracking the boundary conditions. Several researchers have used various types of methods to incorporate the design dependent loads. For eg. Du and Olhoff [14] presented a robust algorithm based on the modified isoline technique that generates the appropriate loading surface during the topology optimization. Seung Ho Ahn et. Al [15] used a level set-based topological to incorporate the design dependent loads. The author embedded the level set function into fixed initial domain to

implicitly represent thermal boundaries. Bruns solved the non-linear steady-state heat transfer using the lumped convection method [16].

But to carry out the thermal topology optimization problem using ANSYS, the conjugate problem is modeled as purely conduction problem. But to still accommodate the convection part and inverse analysis is carried out i.e. the heat source is converted into a heat sink and the heat sink is converted into a heat source. Doing so allows us to solve the conjugate (convection+ conduction) problem as a purely conduction problem [17]. Thus this technique of inverse analysis was used in this thesis.

To perform the topology optimization process, a steady-state thermal analysis had to be carried out. The inner boundary was kept to be insulated while the outer boundary wall was kept at 0 C. An internal heat generation of 100W/m³ was applied to the design space region between the walls. These boundary conditions were applied to depict the problem we were trying to solve- the center of the cylinder being at a higher temperature than the outer walls. The temperature profile achieved is shown under the results section. The boundary conditions for the steady-state thermal analysis are shown in the figure below :-

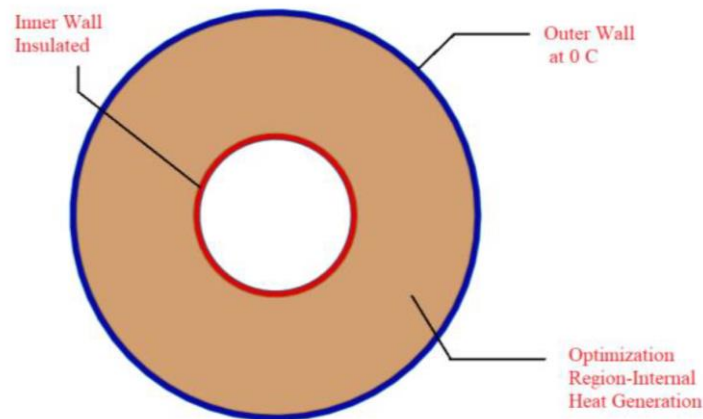


Fig 2 - Steady State Thermal Analysis

The parameters setting for mesh and Steady State thermal analysis are mentioned in the table below:

Table 1 : Boundary Condition for steady state analysis

Boundary Condition	Value
Outer Wall	0 C – Temp
Inner Wall	Insulated (W=0)
Design Space	100 W/m ³ - Internal heat generation
Number of elements in mesh	39,482 elements

The results from the steady-state thermal analysis were used as an input for the topology optimization. The density-based method was used with SIMP to carry out the topology optimization process. The objective function was set to minimize the overall thermal compliance. A mass constraint of 30% was applied to the design space. An external manufacturing constraint of member sizing was added to ensure that no fin goes below a minimum size thickness. The parameters setup for topology optimization are mentioned in the table below:-

Table 2 : Setup Parameters for Topology optimization

Topology Optimization Parameter	Value
Optimization Methods	Density based – SIMP method
Objective function	Thermal compliance
Mass Constraints	30% Volume
Manufacturing Constraint	Member Sizing of -0.8mm
Penalty Factor	3
Convergence Criteria	0.001
Normalized density	0.001

3.2.1 3D Model design

A 2D optimized surface was obtained from the topology optimization process which was then imported into Solid Works to create an optimized 3D model as shown in Fig.3. The results generated from topology optimization are generally not smooth hence proper curve fitting and replacement of unsmoothed curves was done manually using the spline tools. To create the 3D model, the 2D optimized surface was extruded

along a helical path with a straight length of 70mm. The idea behind using a helical path extrude over straight extrude was to increase the overall convective surface area within the same sized domain. It has been observed for a given design having the same mass and similar volume, there was a 19.1% increase in surface area when extruded over a helical path in comparison to a straight extrude. Apart from that, the helical paths provide a larger retention time and help in creating secondary flows which can assist in increasing the overall convective heat transfer coefficient.



Fig 3-Helical Extruded Heat sink

3.2.2 Validation Study

The topology optimized design had to be validated for its thermal performance. A basic study was carried out using the steady-state thermal analysis to analyze the performance of the optimized heat sink design and compare its performance against conventional straight fin heat sink design.

To carry out the comparative analysis only one-fourth of models of the heat sinks were used to reduce the overall computational time. The objective of the validation study was to get a basic idea of which design performed better. To measure the performance, we simulated a heater, and the goal of the heat sinks was to lower the temperature of the heater. Thus, three cases of steady-state thermal analysis were carried out. Case 1 – steady-state analysis of the heater alone without any type of heat sink attached. This was done to establish a baseline value of the heater's surface temperature. Case 2- steady-state analysis of the heater with a straight fin heat sink attached. Case 3- steady-state thermal analysis of the heater with topology optimized heat sink attached.

The boundary condition for all the cases is mentioned in Table 3 below. For Case 1 where the heater was simulated alone, the outer circular wall had a convective boundary condition while all the other walls were adiabatic ensuring the heat transfer occurs only in the radial direction. In the case where the heater was used in conjunction with the heat sinks (Case 1 and Case 2) the fin side walls had a convective boundary condition while the rest of the walls had adiabatic boundary conditions. An Internal heat generation of 12.5 mill/m³ was applied in the heater body simulating an actual heater. (the value was calculated using the data from the cartridge heater being used for experiments).

Table 3: BC for Steady state thermal analysis for Validation study

Boundary Condition	Value
Case 1 - Heater without use of heat sinks	
Inner circular wall , side walls	0 W- Adiabatic
Body	12.5 Mill W/m ³ – internal heat gen.
Outer Circular Wall	30 W/m ² – Convective BC.
Case 2&3- Heater with Straight fin heat sink & Heater with optimized heat sink	
Fin Walls and outer wall	Convective boundary – 30 W/m ²
Heater body	Internal heat gen- 12.5 Million W/m ³
Inner circular wall, side walls	0 W – Adiabatic

To make sure the results from the comparative study are meaningful and can be compared against each other the heat sink design were made such that they had the same weight, similar fin thicknesses, same material, and similar design spaces. Thus, a 3D model of one-fourth straight fin heat sink was designed using 7 fins, with fin thickness of 1.2mm. The material used was copper and the overall weight of the design was 28g approximately. The surface area to volume ratio was 1.67 m⁻¹.

On the contrary a similar model of the topology optimized design had a weight (28 g) and was made of copper. The number of fins and fin thicknesses were nearly the same but varied in geometry. The surface area to volume ratio was obtained to be 2.01 m⁻¹.

The two designs are shown below;

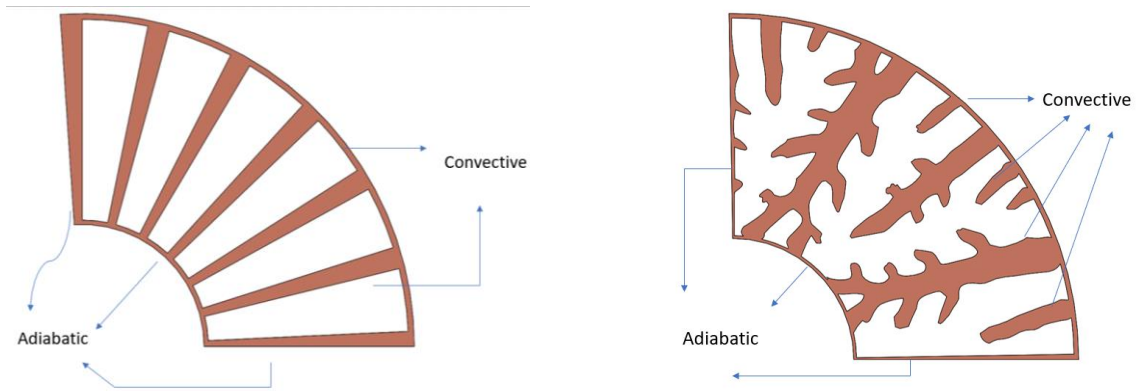
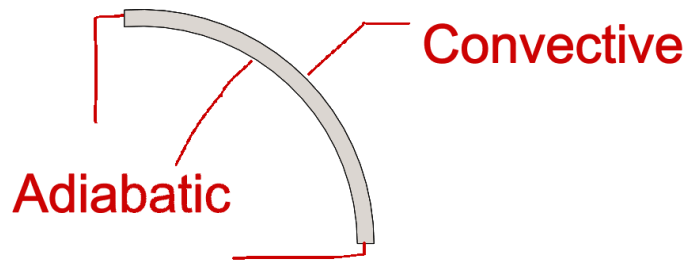


Fig 4- Boundary condition on the a) heater
 b) straight fin c) topology optimized design

Some basic design details for the above designs are mentioned in the table below. All the steady state simulations carried out in this study were done at high mesh counts and mesh independent analysis was carried out for each case which is presented in the results section.

Table 4: Comparative analysis between both heat sink design

Design parameters	Straight fin	Topology optimized
Mass	28.5	28
Fins	7	Approx. 7
Avg. Fin thickness	1.0-1.8 mm	1.5-2.5 mm
3D extrude	10 mm	10mm

Surface Area	5871 mm ²	7425 mm ²
Volume	3431.39 mm ³	3381.5 mm ³

3.3 Additive Manufacturing

The additive manufacturing process used to produce the design was the Fused Filament Fabrication process also known as Fused Deposition Modeling (FDM). The FFF process was used due to its advantage over other additive manufacturing processes like SLS and DED. The FFF process is quite simple to setup and maintain, is cheap, no powder handling, easy removal of supports and no sophisticated laser or powder removal system. The major reason for which the FFF process appeals is its low cost. To 3D print parts made of metal, a special kind of filament has to be used. In our project we have used the Copper-PLA filament produced by the Virtual Foundry.

3.3.1 Copper- PLA filament

The Copper-PLA filament from Virtual Foundry is made of small copper particles mixed with PLA as binder material. The filament contains 90% copper and 10% PLA.

The manufacturing process of the filament is mentioned on the virtual foundry website [18]. Due to the high presence of copper, this filament is quite brittle in nature as compared to other PLA, ABS or nylon filament. Thus extra care must be taken while printing with this filament. The standard diameter is 1.75 mm and it comes in a 1 kg spool. Since the filament is brittle and slight mishandling or straightening can cause the filament to fracture, a Filament Warmer is used. The function of the filament warmer is to preheat the filament, so that the filament loses its shape memory around the spool and becomes soft. Once heated the filament becomes soft and less brittle and can stay in this form for around 24hrs. [18] The preheat temperature is around 53 C. The filament is shown in the figure below.



Fig 5 - Copper- P LA Filament from Virtual Foundry

3.3.2 3D-Printer

The biggest advantage of using virtual foundry filament is that it is compatible with any kind of FDM printer. For our project, we have used the Lultz-bot TAZ-6 printer to print the parts. The CAD model from Solid Works had to be converted into an STL file so that it could be imported into slicing software called CURA. Since this filament is a metallic filament, the printing parameters had to be adjusted to achieve the best results. The ideal printing temperature for this filament was 220 C to 230C. Stainless steel nozzle of 0.6 mm had to be used instead of using the conventional 0.4 mm nozzle. This is because the filament is more viscous compared to a polymer filament and can clog very easily. A major print setting that had to be adjusted was the print speed. Low print speeds were used mainly because of two reasons: 1) To avoid any filament breakage. 2) To provide enough time for the extrude to cool down and solidify before the next layer is printed. The layer height also played an important role in the printing of the part. The lesser the layer height the better and denser parts can be achieved. But as we go below a certain layer height the nozzle starts clogging easily. Thus, in our case, the limiting layer height was around 0.2 mm. A picture of the 3D printer is shown below.

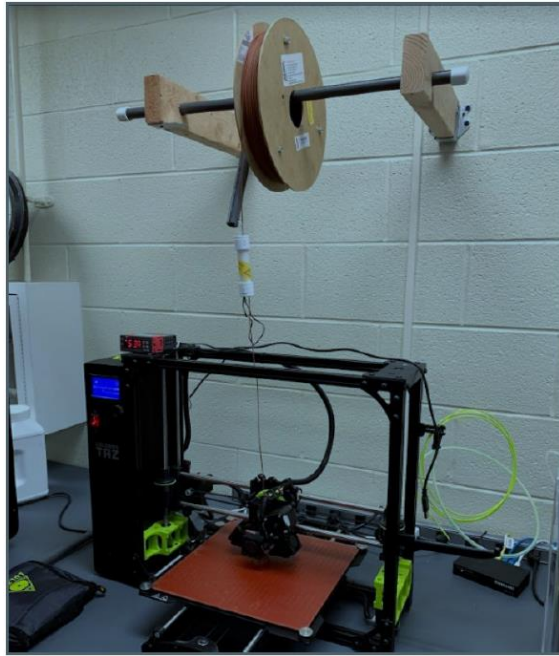


Fig 6 - Lultz—BOT 3D printer with Spool

3.4 Sintering

The “green part” obtained from the 3D printer does not have the same properties as that of pure copper due to the presence of PLA inside the printed part. To achieve parts made of pure copper the “green part” had to be sintered.

This section discusses in detail the various types of sintering processes used and the reason for using them. It also discusses the pre-sintering process of preparing the samples. Finally, we will discuss the post sintering processes done to achieve the heat sink design. The post sintering processes done to achieve the heat sink design.

3.4.1 Sample Preparation

Before carrying out the sintering process, the “green part” achieved from the 3D printing process must be prepared using a Ballast material. The ballast material is added to provide an external support to the part during the sintering process. This is because during the sintering process comprises of two processes a debinding process and a final sintering process. During the de-binding process, the binder inside the green part sublimates and is lost. The loss of binder results in creation of large porosities and loss of

structural strength. If the part is not externally supported the loss of the binder would cause the parts to collapse. Thus proper support using the ballast material must be provided.

In our case, we used CaSO_4 powder as the ballast material due to its ability to produce various concentrations of CaSO_4 solutions. Using the CaSO_4 solutions helped us in reaching the intricate parts within the design quite easily. Also, the CaSO_4 can withstand very high temperatures without degrading. Thus to prepare the sample for sintering, initially a thick paste of 3:1 powder (weight) to water (volume) ratio was mixed and used to seal the bottom of the heat-exchanger. Then a very thin solution of CaSO_4 was used to pour the support material inside the intricate channels. To make sure the solution reaches all parts of the heat sink, the part was regularly tapped and shaken. Lastly, a CaSO_4 solution of 1:1 powder to water ratio was prepared and poured inside the crucible to fill the crucible with the support material. Then slowly and steadily, the semi-covered "green part" was placed in the middle of the crucible to achieve the best possible sintered results. Alternative attempts of using alumina powder as the ballast material for sintering had been attempted but results were quite poor.



Fig 7 - Sample Prepared for sintering.

3.4.2 Sintering Process

To sinter the part the Thermo-Scientific Fisher's Lindberg Blue M Furnace was used. The furnace was equipped with a PID temperature controller and had a max. operating temperature of 1100 C. Several attempts of sintering were carried out. While sintering, it is important to make sure that the part does not oxidize in the presence of air. It is observed that copper at temperature greater than 600 C get oxidized at a uniform rate and thus special care has to be taken[15].

a) Open Environment:

Initially the sintering was carried out in an open environment. Sintering in an open environment is the most common and the easiest form of sintering process and hence it was chosen to be the baseline method of sintering against which other sintering processes could be compared. The sample was prepared and was kept in the center of an alumina crucible. The crucible was then placed inside the furnace on a hearth tray. The sample was initially heated up to a de-binding temperature of 150 C where it was held for 90 minutes. This was done to ensure that the binder material (PLA) completely evaporates from the green part leaving only the metal (Copper) behind. Once the de-binding process was complete, the sample was then raised up to a sintering temperature of 900 C where it was held for another 90 min before quenching it in cold water. Thus a total of complete 9 hour of sintering cycle was used. The temperature profile used in the heating portion of the sintering process is shown in Fig []. The results from the sintering process showed the sintered part was completely oxidized and the hold times were insufficient for proper sintering of copper. Thus a new method had to be devised to carry out the sintering process. These results have been discussed in detail in the upcoming chapter 4.

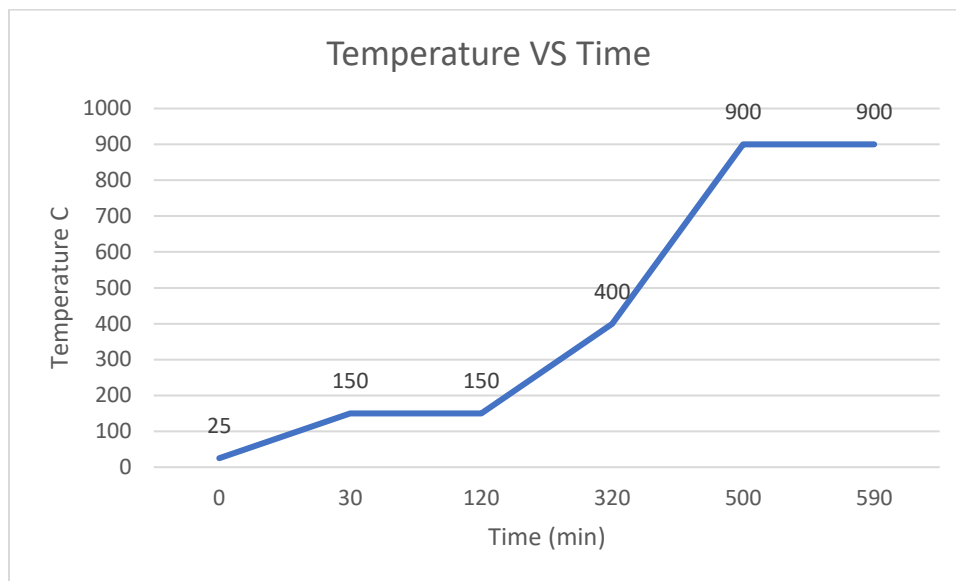


Fig 8 - Temperature(y axis) Vs Time (x axis) for open environment sintering

b) Vacuum Environemnt:

The failure of sintering in an open environment led us to explore other sintering processes. To avoid oxidation (which was the major issue in the previous method) it was suggested that the sintering must be carried out in a vacuum environment. A new sample was prepared and then placed inside a vacuum furnace. A vacuum of 0.2 bar was pulled on the sample to avoid any interaction of air with the copper part. The sintering was done for longer periods of time and at higher temperatures to ensure proper fusion of metal particles. The sintering temperature used was 1000C and the hold time was 4 hrs. The de-binding temperature was 204 C and the hold time at this temperature was 3 hours. Initially the temperature was ramped from 25 C to 204 C in 70 min. The sample was then held at 204 C for 200 min before ramping upto 400 C in 90 min. Without holding, the temperature was then ramped upto 1000 C in 240 mins. At this temperature (sintering temperature) the part was then held for 4 hours and then the furnace was cutoff to let the part naturally cool down to room temperature inside the furnace. The longer hold times were used to allow the parts to be sintered properly. The de-bind temperature was selected to be the glass transition temperature of PLA. The temperature profile used in this sintering process is shown in fig. below. The results from this sintering process showed no signs of oxidation. But due to the

lack of proper support the final shape of the part was distorted. Thus the next step was to test the sintering process in inert environment.

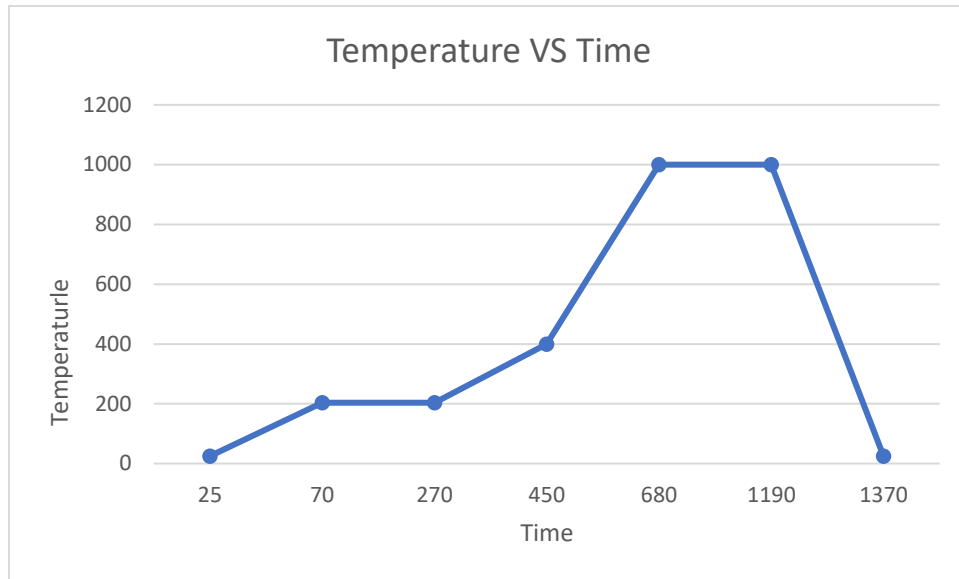


Fig 9 - Temperature Vs Time in Vacuum Environment

c) Inert Environment

Finally the part was also sintered in Inert environment. To sinter the part in inert environment a special type of crucible was designed and manufactured using 316 Stainless Steel. Stainless steel was chosen due to its strength and resistance to oxidation at higher temperatures. The crucible was made from a 2.5 inch diameter tube and flat plate welded to the bottom. A nozzle was welded on the side of the crucible to supply the inert gas. The crucible used is shown in the fig [].



Fig 10 - Crucible for Inert gas sintering

To carry out sintering in an inert environment, Two gases were mainly used helium(He) and Nitrogen(N₂).Initially N₂ gas was chosen as the primary choice of inert gas. An ultra pure N₂ gas cylinder of 200 cuft volume was used for supplying the N₂. The gas was supplied at 30 PSI and 1.5 L/min of average volume flow rate. The flow rate was measured and controlled using a rotameter. A lid was placed on top of the crucible with a 1.2mm hole drilled near the center. The purpose of using the lid was to create a small closed environment with positive pressure inside thus ensuring an air free environment inside the crucible. The small hole drilled on the lid was to avoid any large pressure buildup and to allow trapped gasses to escape.

For the inert environment the temperature profile was further improved. A secondary de-binding step was added.The temperature was intially ramped from 25 C to 204 C in 70 mins. The temperature was then held at 204 C for 2 hrs. The temperature was further ramped upto 483 C at a constant rate of 3C/min where it was then held for another 3 hours. This extra de-bind step was added to confirm that all the PLA is lost before the final sintering step. Next the temperature was ramped upto 1118 C in 5 hours . The rate of ramping was then slowed down. The part was then slowly raised to a sintering temperature of 1170 C where it was held for 3 hours and then slowly allowed to naturally cool down to room temperutre inside the furnace.

A graph depicting temperature vs time is shown below for the inert environment:

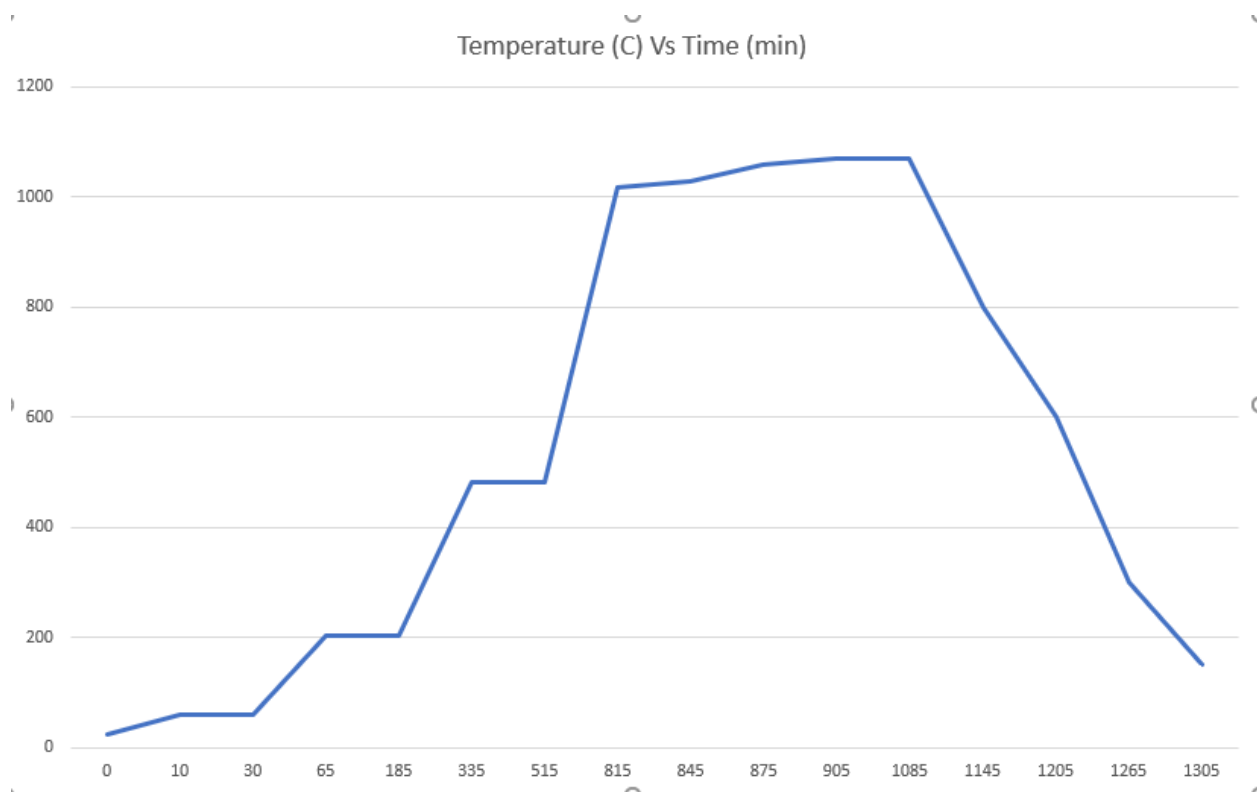


Fig 11 a- Temperature Profile Vs time for Inert Environment

Next the sintering process was carried out using Helium as the inert gas. Since the results obtained from the above temperature profile were quite satisfactory thus the same temperature profile was used. An ultra-pure helium gas tank of 300 cuft was used to supply at a pressure of 30 psi and a flow rate of 4L/min. The results from these sintering process is discussed in detail in chapter 4.

After the sintering is complete and the sample has cooled down, the sample is taken for post processing. In post processing there are mainly two things which must be taken care of. First, to remove the ballast material from the sintered part and second to measure the shrinkage. The sample is placed in a HCL bath to remove the ballast material from the heat sink. It is kept in there for couple of hours and then removed for final polishing. To measure the shrinkage, the final height and the final diameter of the part is measured. The shrinkage is calculated by the formula given below:

$$\frac{\text{Initial length} - \text{Final length}}{\text{Initial Length}}$$



Fig 11 b - Heat sink inside the HCL

3.5 Experimental Setup

In the literature a lot of research can be found on computational analysis of heat sinks , but very little research has been done on the experimental analysis of heat sinks. Thus, an experimental setup must be designed to evaluate the performance of the 3D printed heat sink.

To evaluate thermal performance of 3D printed cylindrical heat sink design an experimental setup was designed using N2 gas cylinder , a small tubular section, thermocouples, cartridge heaters, variable power supply, rotameter and 3D printed support structures. The experimental setup consisted of a tubular test-section made of either copper or ABS material. The tubular section was hollow cylindrical pipe of 22.0 cm in length and 2.7 cm in diameter. The heat sink was placed in the center of this tubular section. The ends of the tube were sealed and capped.

To simulate a hot fluid or a heat source at the center of the heat sink a cartridge heater was inserted inside the heat sink. The heater had a built-in thermocouple inside it and the wires from the thermocouple as well as the main heater wires were extracted through a hole in the cap. The caps were secured and insulated at the ends to ensure no gas leaks. One of the caps had a fixed nozzle drilled into it so that the N2 gas could be supplied through it . The N2 gas was supplied using an Ultra-Pure N2 gas tank at a

delivery pressure of 30 psi. The power inside the heater was controlled using a Variac power supply. The Variac was operated mainly at 20 V and 25 V.



Fig 12 - a) Rotameter b) Helium Gas Tank c) Variac

There were three set of k-type thermocouple installed at different locations along the length of the tube to measure the temperatures. Two of the thermocouple were located on the upstream and downstream side of the heat sink so that they could measure the N₂ gas temperature at the inlet and the outlet of the heat sink and the last thermocouple was placed on the surface of the heat sink to measure the surface temperature. Flow rates of N₂ gas and power of the heater were varied to create different heating and cooling effect through the heat sink. Due to forced convection- the heat sink would cool down and temperatures from the thermocouple were noted. These temperatures were then further used to analyze the performance of the heat sink.

Also, two holes were drilled at the bottom of the tube to measure the pressure drop across the heat sink. A V type manometer was designed with an inclination of 30-33 degrees achieving max. sensitivity in measuring pressure while keeping the design to small. The manometer used WD - 40 as the measuring fluid due to its low density. The pressure drop was measured at high flow rates of 5L/min.

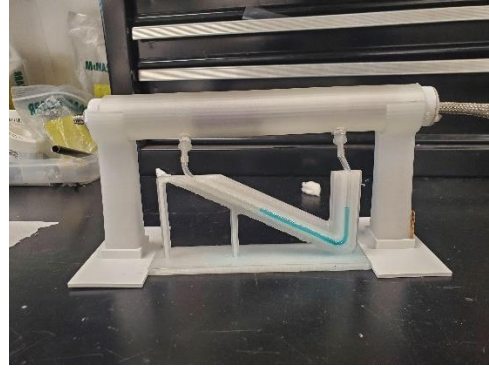
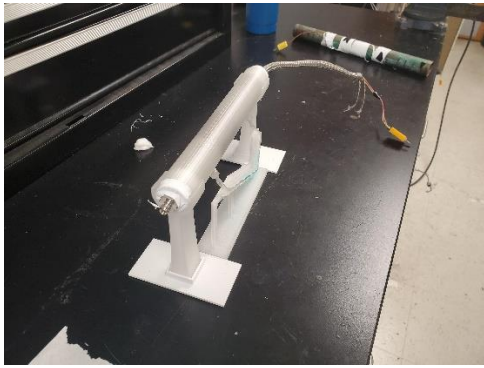


Fig 13 - Picture of Setup with a V- manomter hooked up to measure the pressure drop.

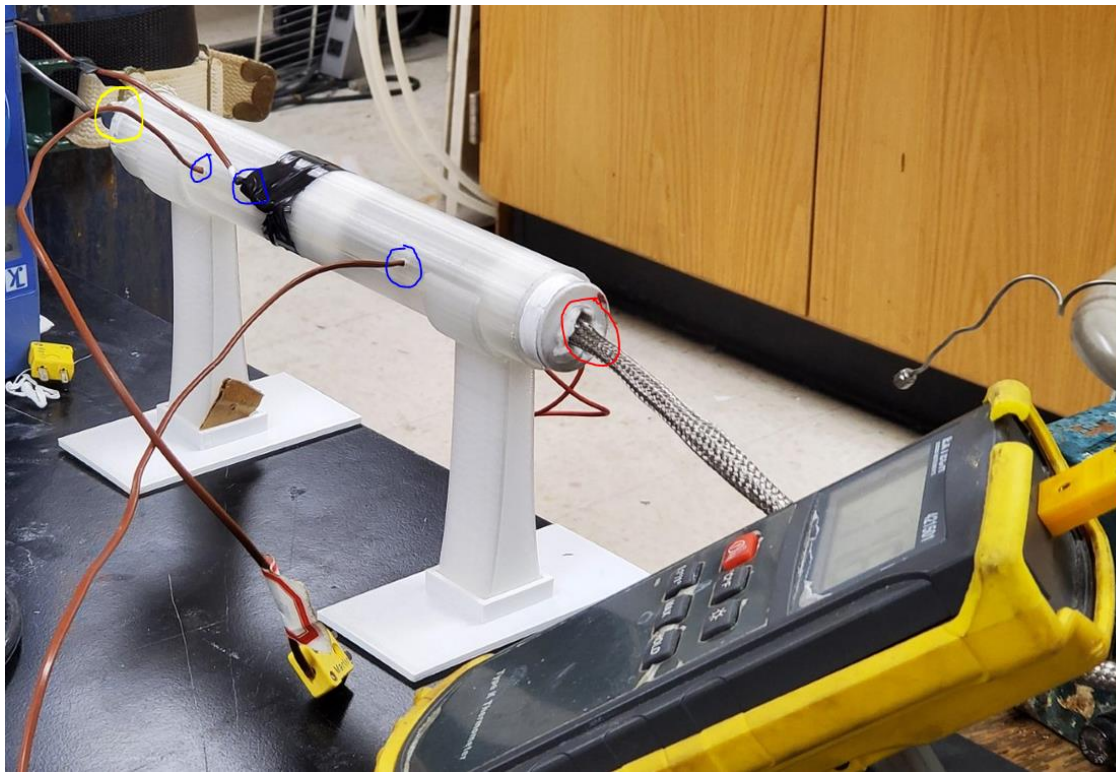


Fig 14 - Picture of the experimental Setup a) The blue circle denote the thermocouple placement b) the red circle denote the heater wire coming out of one end c) The yellow circle denotes the nozzle for N₂ supply.

Chapter 4

Results and Discussion

4.1 Result – Topology Optimization

The results from the steady state thermal analysis showed a temperature gradient across the design domain such that higher temperature regions were found closer to the center and lower temperature regions near the outer boundary of the design space. This was expected and correctly depicted the problem that we were trying to solve i.e. a heat sink with heater in the center.

The results obtained from the topology optimization analysis showed the formation of a dendritic structure emerging from the outer boundaries. These structures moved radially from the outer wall to the center of the design domain. They had smaller branches coming out. The average thickness of each dendritic structure was around 1.2 mm near the outer edge. The formulation of the dendritic structure is quite common in optimized heat sink designs and have also been previously used by other researchers. [16][17][18].

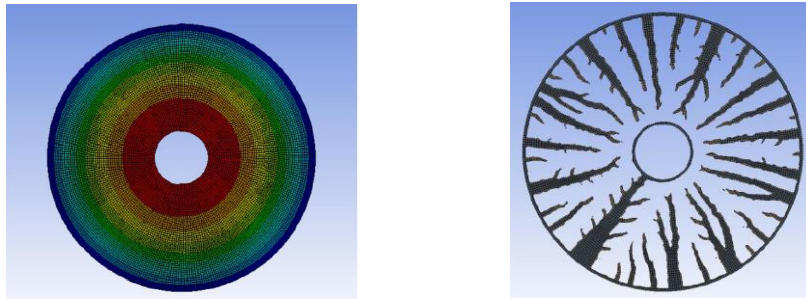


Fig 15 - a) Temperature Profile b) Topology optimized results

The results from the topology optimization had to be extrapolated to meet at the center. The results showed great dependence on the convergence criteria and a 0.001% convergence criteria allowed us to achieve good results.

4.2 Result - Validation study

The result from the validation study was quite promising. They showed that the topology optimized design performed better than the conventional heat sink design. Using a convective boundary condition of $h= 30 \text{ W/m}^2$ on all the fin walls let us simulate a moving fluid. A mesh independent study for each set of the simulation was carried out to verify that the final results were independent of the mesh.

The result of the steady-state thermal analysis of the heater showed that the average surface temperature was around 424.2 C. And such high temperature was expected as the heater had large internal heat generation and only one side to be emitting out heat from the surface. The area available for convective heat transfer is 229 mm². When using a straight-finned heat sink the average temperature of the surface of the heater was reaching to be 43.37 C. The surface area available for heat transfer is 3394 mm². Thus with the large area available for heat transfer the temperature can be expected to be as low as 43.37 C. Finally, the result from the topology optimized design showed that the heater's average temperature on the top surface is 38.4 C using the optimized heat sink design. The results have been highlighted in the table below.

Table 5 : Temperature comparison on the heater surfacec in all 3 cases

Tpye	Mesh	Avg. heater temp (C)
No heat exchgner	976479	424.2
No heat exchanger	1.086 million	423.2
Straight fin	976479	43.37
Straight fin	1.08 Million	43.1
Topology optimized Design	976479	38.4
Topology optimized Design	1.08 Million	38.1

Thus by performing a basic validation study we were able to understand that optimized design did perform better in terms of removing heat.

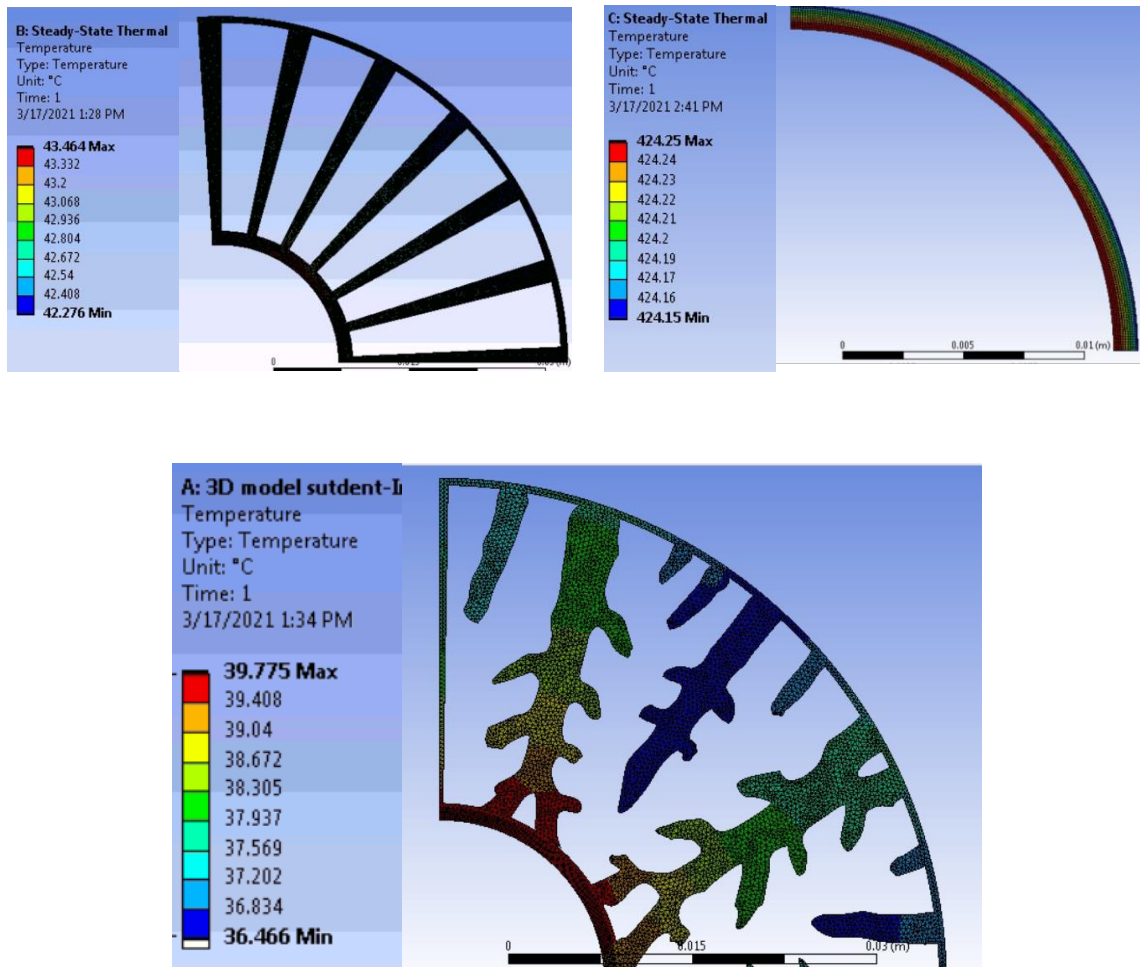


Fig 16 - Temperature distribution a) plain heater b) Heater with straight fin heat sink
 c) Heater with optimized heat sink

4.3 Results - Additive Manufacturing :

The 3D printing process posed several issues initially but then using the optimized parameters mentioned in chapter 3 and taking care of the flow rates we were able to print parts with great accuracy and excellent surface finish. Several pieces of the optimized design and the straight fin design were 3D printed using the Lultz Bot 3D printer. With a layer thickness of 0.25mm, print speeds of 30 mm/s, and a printing temperature of 230 C, the parts were printed smoothly within 4 hrs. None of the parts

required any external supports as they were printed vertically and there were no overhang structures. For proper Bed adhesion and easy removal of part a raft was added to each print. While printing it was made sure the filament was positioned right above the printer and that there was no extra tension in the filament that could cause the filament to break. The printed parts had smooth textures and printed quite accurately and are shown in the fig below.

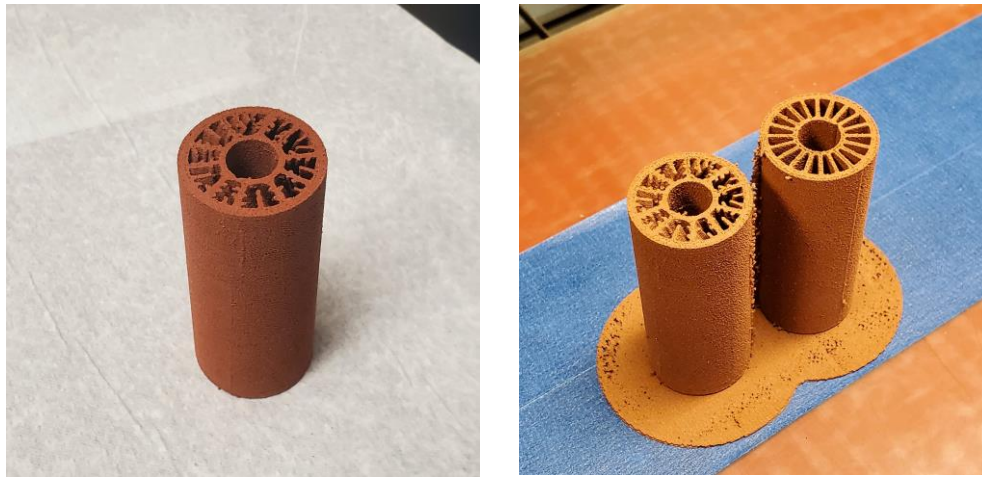


Fig 17 - 3D printed on Lultz Bot 3D printer

4.4 Results - Sintering Process

Results from the open environment sintering process were not that successful but it gave us some idea about the temperature profile and process needed to be carried out . The major issue found in the open environment sintering was that of oxidation. Severe oxidation of copper took place which resulted in the formation of black copper oxide. The copper oxide was highly brittle, non-conductive and would crumble with slight handling. Thus, the overall structural integrity and functionality of the part was all lost.

Also, it was observed that there were large pores and gaps in the design showing that the part did not have enough time to sinter properly. In fact, the sintering temperature had not been reached during the process. The resulted samples are from open environment sintering are shown below.



Fig 18 - Sintered parts- From open environment.

The next step in the process of carrying out sintering was to carry out the sintering process in Vacuum environment . This was done majorly to reduce the oxidation of copper during the sintering process. Also, as we had realized that we needed longer sintering periods , a new temperature profile was prepared. The total time for the sintering cycle increased from 9 hrs to 17 hrs (approx.).

The vacuum sintered part produced was good successful part as it did not show any kind of oxidation on its surface. The part produced was heavy, hard and sonorous and had a really copper like shine. The only issue was that there were large discontinuities on the surface and the reason for that being was the lack of proper support material. So during the sintering process when the binder material sublimates the copper particle does not have much of strength to withstand on its own and this requires proper support. Lack of support can result in the walls to droop and have a rough texture which was seen in this case.

To just test if there is formation of oxides we did a basic electrical conductive test. Done at various location the conductivity test showed that the part was made of pure copper.



Fig 19 - Sintered part from Vacuum Furnace

The final process was the sintering using the inert gas. To tackle the issue of creating large Vacuum requiring expensive furnace and getting better surface finish the final sintering process was done in the inert . Several parts were sintered testing the inert gas environment multiple times. The results from the sintering process in inert environment is promising. Two inert gases were used for sintering the part. To sinter the part in the inert environment a special type of crucible was designed as mentioned in chapter 3. First the parts were sintered in N₂ environment. The crucible with the nozzle was attached to N₂ tank and an average flow rate of 1.5 L/min was maintained inside the crucible. The rotameter measured the flow rate.

The sintered part achieved after going through a 24 hours thermal cycle was quite promising. The part had very less oxidation on the surface. Only little part at the bottom had been oxidized. But the oxidation was not up to the level that would make the part useless. But on the other hand, the part was well supported and had a good surface finish and was able to maintain its structural integrity.



Fig 20 - Part Sintered in N₂ gas

Lastly , the best results for sintering were obtained using helium as the inert gas. Helium being lighter than air acts as a shield on top of the sample parts and thus not let the air reach the inside of the sample.

Helium was used at flow rates close to 4 L/min. Basic calculations of the flow rate and time to run the experiments were done to ensure that the experiment does not run out of Helium gas. The result obtained by using helium as the inert gas were quite promising. Two sintering process on straight fin design of heat sink were carried out.

The results showed no signs of oxidation in any case on the surface. On the contrary the stainless-steel crucible since undergoing several sintering cycle had been oxidized to some extent due to which the oxides of iron had been deposited on the surface. The surface morphology was far better than the Vacuum furnace and showed very less discontinuity. The slight gaps in the wall are due to the presence of iron oxide. If the crucible were in good condition this would have not occurred.



Fig 21 – Sintered part from Helium gas sintering

Shrinkage was a major factor. The shrinkage was predetermined to be 15 % and the design had been sized accordingly.

4.5 Results - Experimental Setup

The results from the experimental setup were taken in terms of temperature and pressure profile. The goal here is to use those results to finally calculate the effective thermal conductivity of the heat sink. Four thermocouples were used to measure the temperature at various location. One thermocouple measured the temperature at the center (at the heater surface or at the core).This was the in-built thermocouple. The values of this was thermocouple was the primary temperature source. The second thermocouple was attached at the surface of the heat sink. The other two thermocouple were attached to measure the temperature of nitrogen prior to entering the heat sink and the temperature after it comes of the heat sink. For our purpose we will use the temperature at the center and at the surface of the heat sink to calculate the effective thermal conductivity.

The temperature results obtained from the experiments for no flow, and flow at 1 .5 L/min , 2 L/min etc are listed in the table below. The power was adjusted and controlled using a Variac. The resistance of the heater is known to be 70 ohms.Thus results for two different POWER is tabulated.

Power – 20 V and current – 0.36 – $P = 20 \times 0.36 = 7.2W$

Table 6 : Temperature profile along the test sections @ 7.2 W

Voltage (V)	Current (I)	Power (W)	T center	T surface	T 1 - upstream	T 2- downstream	
20	0.36	7.2	117	72	34	45	Without N2
20	0.36	7.2	112	71	27	47	N2 -1.5 L/min
20	0.36	7.2	105	65	26	46	2 L/min
20	0.36	7.2	97	61	25	42	3 L/min
20	0.36	7.2	91	55	25	42	4 L/min

Table 7 : Temperature Profile along the test section @ 10.5 W

Voltage	Current	Power	T center	Tsurface	T1 upstream	T2 downstream	L/min
25	0.41	10.25	161	92	44	55	2
25	0.41	10.25	149	85	25	63	3
25	0.41	10.25	137	72	24	61	4
25	0.41	10.25	126	70	24	71	5

4.5.1 Calculation of effective thermal conductivities

To characterize the thermal performance of the heat sink design we need to find a quantity which can be directly used to compare various design. The ideal way of characterizing the heat sink design would be by calculating the Coefficient of performance or in other words the efficiency of heat transfer. In many situations calculating the COP is little hard and thus alternative methods of comparing the performance must be found. One way of comparison would be to compare the temperature drop achieved across the heat sink's core and the surface for a given set boundary conditions. But this is quite a vague method and could vary differently in different regions of the design.

Another method of evaluating the performance is by calculating the effective thermal conductivity or bulk thermal conductivity. The bulk/effective thermal conductivity is generally calculated for porous media and thus can be extended here[24][25][26]. The effective thermal conductivity will be calculated as normal thermal conductivity of any solid body, but this thermal conductivity will contain the effect of convection also within it. It is not to be confused with the actual thermal conductivity of a body which is constant and is a property of the material. But infact the effective thermal conductivity for a body can change and increases with increase in overall convective heat transfer.

To calculate the effective thermal conductivity in our case the Fourier's Law for hollow cylindrical body was used. From Fourier's Law we have :

$$\dot{Q} = 2k\pi\ell \frac{T_1 - T_2}{\ln(r_2/r_1)}$$

Rearranging the equation $k = \frac{\ln\frac{r_2}{r_1} \cdot Q}{2 \cdot \pi \cdot l \cdot (T_1 - T_2)}$


In the equations used above r1 is the inner radius, r2 is the outer radius, l is the length of the heat sink and T1 and T2 are the heater temperature and surface temperature, respectively. This equation is derived by solving 1D problem in cylindrical coordinate.

The results from the table 6 and 7 were used and put in an excel sheet to calculate the effective thermal conductivities at various flow rates. The effective thermal conductivities calculated for various flow rates are shown in the figure below. This effective thermal conductivity can be used to compare the performance of two heat sink design.

Power =10.25 W

flow in L/ min	V	I	Q (W)	T _{outer}	T _{inner}	ln(r2)/r1	DT	2*pi*L	K
2	25	0.41	10.25	92	160	1.014147	68	0.4396	0.347743
3	25	0.41	10.25	85	149	1.014147	64	0.4396	0.369477
4	25	0.41	10.25	72	137	1.014147	65	0.4396	0.363792
5	25	0.41	10.25	70	126	1.014147	56	0.4396	0.422259

Power =7.2 W



Flow in L/min	V	I	Q	T _{outer}	T _{inner}	Ln(R2/r1)	DT	2*pi*L	K
1.5	20	0.36	7.2	72	117	1.014147	45	0.4396	0.369116
2	20	0.36	7.2	71	112	1.014147	41	0.4396	0.405127
3	20	0.36	7.2	65	105	1.014147	40	0.4396	0.415256
4	20	0.36	7.2	61	97	1.014147	36	0.4396	0.461395
5	20	0.36	7.2	55	91	1.014147	36	0.4396	0.461395

Fig 22 - Effective Thermal Conductivity

4.5.2 Measuring and Calculating the pressure drop

Measuring the pressure drop across the length of the heat sink is of great importance especially in places where the heat transfer takes place between two fluids in a long heat sink. The larger the pressure drop the greater pumping power would be required. Thus, lower pressure drops are always desired. But in cases where the surface area for heat sink is increased the overall pressure drop across the heat sink increases. In our case we have calculated the pressure drop to denote that the increase in pressure drop is quite less and insignificant in comparison to the improvement in performance achieved.

The pressure drop is measured using a self-designed V- manometer. The manometer was 3D printed and pipe tubing was added to it. As mentioned in chapter 3 that the V manometer was designed at an angle of 33 degrees. To measure the pressure the value of the fluid displaced is measured. Then using the equation below the final pressure drop can be measured.

$$\Delta P = L \times \sin\theta \times g \times (\delta_{wd} - \delta_{n2})$$

This equation can be derived from any standard manometer design text book or fluids book. The θ here represents the manometer angle , g represents the gravitational acceleration, δ_{wd} represents the density of WD 40 and δ_{n2} represents the N2 gas density. Therefore, if the known values are put in the equation then the equation can be reduced to

$$\Delta P = L \times 4407.7 \text{ pa}$$

Thus, from the experiment carried out, at a flow rate of 5L/min a 6mm of displacement was observed. Based on that, the value of the pressure drop was around 26 pascals which is quite insignificant.

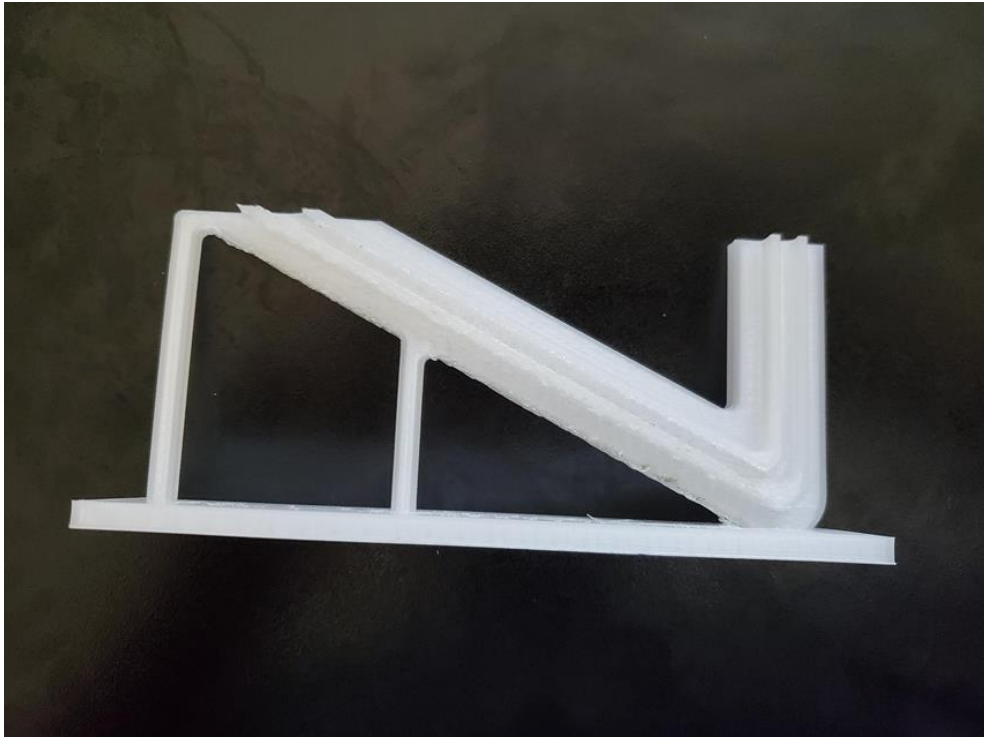


Fig 23 – V-Manometer Design

Chapter 5

Summary

This thesis discusses the design and topology optimization of a cylindrical heat sink design using the ANSYS workbench software. It presents a novel approach of carrying out the thermal topology optimization analysis using the ANSYS workbench software. To model the conjugate problem in ANSYS workbench the inverse analysis methodology was used. The heat source was treated as a heat sink and the heat sink (body of the heat sink) was treated as a heat source. To achieve the topology optimized design an internal heat generation was applied to the whole body simulating it as a heat source. This method is unique and assists in carrying out the topology optimization for conjugate problems without solving for the convective boundary condition at each stage.

The optimized results were then used to create a 3D model of the heat sink design having a helical extrude. The 3D model was then successfully printed on a Lultz- Bot 3D printer using a copper-PLA filament. The printing parameters had to be adjusted to account for the viscous and brittle nature of the filament. The 3D printed part was then sintered in various sintering environments to achieve parts made of pure copper.

Before the sintering process is carried out CaSO₄ Solution was used as the primary ballast material for providing support to the green parts during the sintering process. The open environment sintering did not prove to be quite successful as the sintered parts were majorly oxidized. The results from the vacuum environment showed a great level of improvement in the sintering results. Part obtained from the vacuum sintering process showed no signs of oxidation, but the structural integrity of the part was slightly compromised. The sintering process carried out in the inert environment proved to be the most successful of all the processes as it was able to retain the original shape of the part as well as avoid oxidation. Amongst the inert environment, the results from both N₂ gas and Helium gas were quite good but the results from helium gas slightly outperformed the results from the nitrogen gas. The sintered parts were then

put in HCL baths to remove the ballast material from it. A shrinkage of 15 % percent was observed in all the parts.

To characterize the thermal performance of the heat sink, initially, a comparative study was carried out between straight fin heat sink design and topology optimized heat sink design. The results from the study depicted 12% lower temperatures for parts using the optimized design in comparison to when using a straight fin heat sink design. Also, to further analyze the performance of the heat sink experimental setup was created to measure the pressure drop and the temperature profile of the part. The results were then successfully used to calculate the effective thermal conductivity of the optimized heat sink. The effective thermal conductivity varied from 0.34 to 0.46 W/mK depending upon the amount of heat supplied and the flow rate. The pressure drop was measured and calculated to be around 26 pascals which were quite negligible.

Chapter 6

Future Work

The research work presented in this thesis poses great potential for future research. For instance, it discusses in detail the new method of manufacturing metallic parts using FDM printing as compared to the conventional manufacturing processes of SLS or SLM processes. The next step in this research would be to characterize the printed parts by measuring its porosity and strength features. Although some past work has been done on this more research is needed in characterizing the porosity of the printed parts. Also, the effect of printing parameters on the sintering process could be studied.

A major process discussed here is the sintering process. The next step in the sintering process would be to experiment with the temperature profile of the sintering process and try to reduce the overall time required to carry out the sintering. That means new temperature profiles must be generated. Furthermore, it is important to characterize the results in a more quantifiable manner rather than just a qualitative analysis. For this the level or degree of oxidation in parts can be measured and studied. Also, studying the extent of porosity would be helpful in analyzing the overall thermal conductivity of the part.

At last the performance of the heat sink can be measured by calculating the coefficient of performance (COP). This research does not include the experimental comparison with other conventional design of the heat sinks. This is something which can be done as a part of future work.

Chapter 7

References

1. Ian Gibson David Rosen & Brent Stucker “ Additive manufacturing Technologies – 3D printing, Rapid Prototyping, and Direct Digital Manufacturing” Book II Edition, (2015).
2. Peter VerVoot “Sintering conditions - What to expect from a modern sintering furnace” European PM Conference (2015).
3. Wu, Yifei ¹ ;Jia, Wei ¹ , “Thermal Optimization Design of Heat sink in Supersonic Engine with Parameters' Fluctuation” International Journal of Turbo and Jet Engines, 2020; ISSN: 03340082, E-ISSN: 21910332; DOI: 10.1515/tjj-2020-0013
4. Tuyen, Vo 1 ; Van Hap, Nguyen 2 , 3 ; Phu, Nguyen Minh 2 , “Thermal-hydraulic characteristics and optimization of a liquid-to-suction triple-tube heat exchanger” Thermal Engineering, v 19, June 2020; ISSN: 2214157X; DOI: 10.1016/j.csite.2020.100635; Article number: 100635; Publisher: Elsevier Ltd
5. Oćoń, Paweł 1 ; Łopata, Stanisław 1 ; Stelmach, Tomasz 1 ; Li, Mingjie 2 ; Zhang, Jian-Fei 2 ; Mzad, Hocine 3 ; Tao, Wen-Quan 2 ; “Design optimization of a high-temperature fin-and-tube heat exchanger manifold” Energy, v 215, January 15, 2021; ISSN: 03605442; DOI: 10.1016/j.energy.2020.119059; Article number: 119059
6. Joe Alexandersen, Ole Sigmund, Niels Aage “Large scale three-dimensional topology optimization of heat sinks cooled by natural convection” (2016).
7. Younghwan Joo, Ikjin Lee, Sung Jin Kim “Topology optimization of heat sinks in natural convection considering the effect of shape-dependent heat transfer coefficient”2017.
8. H. Peter de Bock “ Exploration of a Hybrid Analytical thermal topology optimization method for an additively Manufactured Heat Sink”. Aero- thermal organization , GE Global research. (2018)
9. Z.Gobetz, A. Rowen, C. Dickman, K.Meinert and R. Martukanitz. “Utilization of Additive Manufacturing for Aerospace Heat exchanger- Office of Naval research.” (2016).
10. Xiang Zhang, Ratnesh Tiwari, Amir H. Shooshtari*, Michael M. Ohadi “An additively manufactured metallic manifold-microchannel heat exchange for high temperature applications”Journal of Applied thermal engineering (2018).
11. Rachel Ann Felber Gregory Nellis Natalie Rudolph “Design and Modeling of 3D-Printed Air-CooledHeat Exchanger” International Refrigeration and air conditioning conference (2016).
12. M. Pelanconi, M. Barbato S. Zavattoni G.L. Vignoles A. Ortona “Thermal design, optimization and additive manufacturing of ceramic regular structures to maximize the radiative heat transfer” Material & Design (2019).
13. Oyetudun Isaac Aryaani “ Sintering and Characterization of 3D printed Bronze Metal Filament “ Purdue University Master’s thesis.

14. J. Du and N. Olhoff, Topological Optimization of Continuum Structures with Design-Dependent Surface Loading—Part I: New Computational Approach for 2D Problems, *Struct. Multidisc. Optim.*, vol. 27, pp. 151–165, (2003)
15. Seung-Ho Ahn & Seonho Cho “Level Set–Based Topological Shape Optimization of Heat Conduction Problems Considering Design-Dependent Convection Boundary, *Numerical Heat Transfer, Part B: Fundamentals*, 58:5, 304-322. (2010)
16. T. E. Bruns, Topology Optimization of Convection-Dominated, Steady-State Heat Transfer Problems, *Heat Mass Transfer*, vol. 50, pp. 2859–2873, (2007).
17. Ercan (Eric) Dede, “ Multiphysics Topology Optimization of Heat Transfer and Fluid Flow Systems” COMSOL user Conference. (2009)
18. The Virtual Foundry “<https://www.thevirtualfoundry.com/help>” .
19. V V Belousov and A A Klimashin “High-temperature oxidation of copper” *Russian Chemical Reviews*. Rev 82 273. (2013)
20. Gilho Lee, Ikjin Lee, Sung Jin Kim “Topology optimization of a heat sink with an axially uniform cross-section cooled by forced convection” *International Journal of heat and mass transfer* , Volume 168 , April (2021).
21. Fraunhofer IAPT institute “Design better devices — faster” *IEEE Spectrum* 2020
22. Bin Zhang , Jihong Zhu , Limin Gaod “Topology optimization design of nanofluid-cooled microchannel heat sink with temperature-dependent fluid properties” *Applied thermal engineering* Vol 176 (2020).
23. Patil, S., Chintamani, S., Kumar, R., and Dennis, B. H., 2016. “Determination of orthotropic thermal conductivity in heat generating cylinder”. *International Mechanical Engineering Congress and Exposition, American Society of Mechanical Engineer*, pp-V011T15A016 doi:10.1115/IMECE2016-67918 . (2016)
24. Fabela, Oscar, Patil, S., Chintamani, S., and Dennis, B., 2017. “Estimation of effective thermal conductivity of porous Media utilizing inverse heat transfer analysis on cylindrical configuration”. *ASME 2017 International Mechanical Engineering Congress and Exposition*, pp-V008T10A089-V008T10A089 doi:10.1115/IMECE2017-71559.(2017)
25. Upreti R., Chintamani S., Patil S., Akbariyeh A, Dennis B. 2021 , "Stochastic finite element thermal analysis of ball grid array package", *Journal of Electronic packaging*. doi: <https://doi.org/10.1115/1.4050696>. (2021)